Dynamic stability of mineral-associated organic matter: enhanced stability and turnover through organic fertilization in a temperate agricultural topsoil

Marius Mayer [a], Jens Leifeld [b], Sönke Szidat [c], Paul Mäder [a], Hans-Martin Krause [a], Markus Steffens [a,d,*]

[a] Research Institute of Organic Agriculture FiBL, Ackerstrasse 113, CH-5070 Frick, Switzerland
[b] Agroscope, Climate and Agriculture Group, Reckenholzstrasse 191, CH-8046 Zurich, Switzerland
[c] Department of Chemistry, Biochemistry and Pharmaceutical Sciences & Oeschger Centre for Climate Change Research, University of Bern, Freiestrasse 3, CH-3012 Bern, Switzerland
[d] Institute of Geography, University of Bern, Hallerstrasse 12, CH-3012 Bern, Switzerland

ARTICLE INFO

ABSTRACT

Soil organic matter (SOM) plays a vital role for soil quality, sustainable food production and climate change mitigation. It is common knowledge that SOM consists of different pools with varying qualities, quantities, and turnover times. However, it is still poorly understood how mineral and organic fertilization affects the formation and stabilization of mineral-associated organic matter (MAOM) and how long it can remain there. Here, we report on the long-term effects of different farming systems on the stability and turnover of the fine silt and clay-sized MAOM fraction (<6.3 μm) of a Haplic Luvisol (0–20 cm) in the DOK long-term trial (Switzerland). We compared three farming systems with contrasting fertilization (CONMIN = pure mineral, CONFYM = mineral + organic, BIODYN = pure organic) with an unfertilized control (NOFERT) between 1982 and 2017. We performed specific surface area (SSA) measurements on fractionated MAOM samples (<6.3 μm) from 1982 to 2017, before and after removal of OM, measured the ^{14}C activity of all samples during the entire period and estimated the mean residence time (MRT) with a model taking into account 'bomb ^{14}C' and radioactive decay. We found constant MAOM-C contents under organic fertilization. Results of SSA analysis indicate best conditions for MAOM-C stabilization under organic fertilization and different sorption mechanisms in MAOM between farming systems with and without organic fertilization. The modelled MRTs were significantly higher in NOFERT (238 ± 40 yrs) and CONMIN (195 ± 27 yrs), compared to CONFYM (138 ± 18 yrs) and BIODYN (140 ± 19 yrs), implying a high C turnover (i.e. more active MAOM) at high C contents under organic fertilization. Our findings show that MAOM is not the dead OM but corroborates the concept of 'dynamic stability'. Continuous OM inputs from organic fertilizers and their rapid and constant turnover are needed to stabilize the "stable" MAOM-C fraction.

1. Introduction

Arable soils have a large potential to sequester carbon (C) as soil organic matter (SOM) (Amelung et al., 2020; Lal et al., 2018), making this process and the associated measures an attractive negative emission strategy (Paustian et al., 2019). This has prompted scientists and policy makers worldwide to promote it as a strategy for mitigating climate change (de Vries, 2018; Minasny et al., 2017).

SOM has positive effects on many physical, chemical and biological soil properties. Increasing SOM contents in arable soils enhances water holding capacity, soil structure, nutrient cycling and microbial diversity (Lal, 2020; Rabot et al., 2018; Weil and Magdoff, 2004), improving soil fertility and soil health (Bünemann et al., 2018), and consequently contributing to sustainable crop production and food security (Lal, 2010). By improving soil structure, SOM promotes infiltration and retention of water, thus ensuring soil functions in the face of increasing weather extremes (e.g. droughts) (Kundel et al., 2020).

Anthropogenic climate change is predicted to accelerate the already

severe SOM losses (Riggers et al., 2021; Wiesmeier et al., 2016) brought on by land use change and agricultural management (Paustian et al., 2016; Sanderman et al., 2017). Accordingly, it is essential to implement agricultural practices that increase the transfer of atmospheric C to the soil and prevent its rapid release, i.e. promote long-term C storage in the soil as SOM. The application of organic fertilizers is known to enhance SOM contents compared to mineral fertilization (Gattinger et al., 2012; Krause et al., 2022). While fertilizer type (i.e. mineral vs. organic) and qualitative differences between organic fertilizers have shown to be decisive for the accumulation of labile OM (Mayer et al., 2022), their effects on the stable OM fractions remain poorly understood. Therefore, estimating the duration of C storage and understanding the underlying soil processes under contrasting fertilization, especially over long-term periods, is of great interest for the design of the respective measures.

The persistence of SOM, i.e. SOM longevity as a result of the interactions with its chemical, physical and biological environment (Schmidt et al., 2011), can be expressed as mean residence time (MRT). The estimation of MRT is often based on isotopic approaches. Among these, radiocarbon analysis is a unique technique that enables the determination of C dynamics in soils on decadal to millennial timescales (Paul et al., 1997; Trumbore, 2009; Wang and Hsieh, 2002). In mineral soils, MRT of SOM largely depends on organo-mineral interactions, which are driven by specific stabilization mechanisms. Sorption of SOM onto surfaces of fine-sized mineral particles following microbial transformation is considered a dominant mechanism responsible for the formation of a stable mineral-associated OM (MAOM) fraction (Cotrufo et al., 2013; Newcomb et al., 2017; Schmidt et al., 2011). Over time, the gradual formation of organo-mineral complexes and microaggregates (Totsche et al., 2018) spatially separates SOM from microbes and enzymes. This limits its further decay through reduced accessibility and oxygen supply, ultimately increasing the MRT to time-scales of centuries to millennia (Kleber et al., 2015; Kögel-Knabner et al., 2008; Six et al., 2002; von Lützow et al., 2006).

Reactive surfaces of fine mineral particles stabilize the majority of organic C in many mineral soils (Kramer and Chadwick, 2018), but the size of these surfaces varies for different phyllosilicates (Kleber et al., 2021). Therefore, soil mineralogy has a major influence on the SOM stabilization potential (Barré et al., 2014; Feng et al., 2013). However, the dynamic nature and reversibility of this binding mechanism has been described (Kleber et al., 2021; Kuzyakov et al., 2000; Steffens et al., 2009), defying the long-held belief that adsorption to fine mineral surfaces would put a stop to the cycling of affected SOM. In addition, studies dealing with OM storage in differently stable SOM fractions even indicate that this stable MAOM is not increased but only kept stable under specific agricultural practices (Chung et al., 2008; Gulde et al., 2008; Steffens et al., 2011). An improved knowledge of the involved mechanisms will thus allow to better evaluate farming systems in terms of their effectiveness for the long-term storage of atmospheric CO_2 as SOM, thereby maintaining soil quality and contributing to climate mitigation via climate-smart agricultural practices (Paustian et al., 2016).

The objective of this study was to assess the long-term effect of different farming systems on the stability of fine silt and clay-sized MAOM (<6.3 μm; 0–20 cm depth), in the DOK long-term experiment (Therwil, CH) (Mäder et al., 2002). Our study focused on four farming systems: an organic system using only organic manure (BIODYN), two conventional systems, one using only mineral fertilizer (CONMIN) and the other combining the use of mineral fertilizer and farmyard manure (CONFYM), and an unfertilized control (NOFERT). Recent results on the long-term development of bulk SOC (<2 mm) show an increase in BIODYN, no change in CONFYM and decreases in CONMIN and NOFERT (Krause et al., 2022). However, no quantitative changes of MAOM were measured over a 36-year period, regardless of fertilizer quality within the farming systems (Mayer et al., 2022).

We hypothesize, that (i) long-term organic fertilizer application (CONFYM and BIODYN) initiates higher stability of MAOM through enhanced microbial activity and diversity, and as a result (ii) this would translate to longer MRTs than in farming systems with pure mineral (CONMIN) or without any fertilizer application (NOFERT). To test this hypothesis, we measured changes in SSA via N_2 adsorption and took advantage of ^{14}C radiocarbon analyses to elucidate the turnover dynamics within MAOM by means of MRT estimation.

2. Materials and methods

2.1. Experimental setup and sample selection

The DOK farming system comparison trial is located in Therwil (canton of Basel Landschaft, Switzerland, 47°30′ N, 7°32' E) and was initiated in 1978 (Mäder et al., 2002). Here, organic and conventional farming systems are compared under temperate climatic conditions (10.5 °C mean annual temperature; 840 mm mean annual precipitation (Krause et al., 2020);). The soil is a Haplic Luvisol (WRB, 2015), developed on deposits of alluvial loess, with 3% sand, 76% silt and 21% clay (Mayer et al., 2022).

The experiment has a split-plot design, each farming system is replicated in four columns, and subject to the same seven-year crop rotation (crop rotation period = CRP) with two years of grass-clover ley (Supplementary Table 1), temporally shifted in three subplots. All farming systems have the same type of tillage (moldboard plowing, 0–20 cm), but receive different types of plant protection (Supplementary Table 2). We focused on four farming systems with different fertilizer types and quantities within the six completed CRP (CRP 1 = 1978–1984, CRP 2 = 1985–1991, CRP 3 = 1992–1998, CRP 4 = 1999–2005, CRP 5 = 2006–2012 and CRP 6 = 2013–2019). NOFERT is the unfertilized control. CONMIN is conventionally managed, and receives mineral fertilizer only (unfertilized in CRP 1). CONFYM is an integrated conventional system, with combined mineral and organic fertilizer application. BIODYN is an organic, biodynamically managed farming system that receives only organic fertilizer.

In CONFYM (stacked farmyard manure and slurry) and BIODYN (composted manure and slurry), the addition of organic fertilizer is equivalent to the manure and slurry produced by 1.4 livestock units ha^{-1} yr^{-1}. Farming system-specific preparation of raw manures (CONFYM = manure stacking, BIODYN = aerobic composting) led to quantitative and qualitative differences at the time of its application. In addition, slurry is added to meet the nutrient requirements of the respective crop (mainly N). In CONMIN and CONFYM, mineral fertilizers are added up to the limits of Swiss fertilization recommendations (Richner and Sinaj, 2017). Because farmyard manure N inputs are not fully accounted for as readily bioavailable, N inputs are higher in CONFYM than in CONMIN (Supplementary Table 3). After harvest, straw biomass was removed from the plots. Over the observational period from 1982 to 2017, annual OM inputs via manure and slurry to the analyzed plots in subplot B (Supplementary Fig. 1) averaged 2508 (CONFYM) and 2000 kg dry matter ha^{-1} yr^{-1} (BIODYN). Organic and conventional farming systems of the DOK trial have yield-independent belowground C inputs, as well as similar total root biomass and rhizodeposition for the crops present on the analyzed plots in this study (Hirte et al., 2018a; Hirte et al., 2018b). After harvest, straw biomass was removed from the plots.

We used air-dried (40 °C) and sieved (<2 mm) bulk soil samples from the DOK soil sample archive at Agroscope Reckenholz. These were taken from 16 plots (subplot B, see Supplementary Fig. 1) in the same year within each completed CRP (1982, 1989, 1996, 2003, 2010 and 2017) (Supplementary Table 1) after harvest with a soil corer (0–20 cm depth). This totaled 96 soil samples (four farming systems x four replicates x six CRPs).

2.2. Clay content and clay mineralogy

Texture of bulk soil samples (<2 mm) was measured with the PARIO

Plus Soil Particle Analyzer (METER Group, Germany/USA). Prior to measurement, OM was removed from 25 to 30 g of soil via oxidation (12 h) with hydrogen peroxide (H_2O_2, 30%). Subsequently, H_2O_2 was removed from the sample by rinsing with deionized water, centrifuging and decanting until an electrical conductivity of <400 μS m^{-1}. Sodium hexametaphosphate ($Na_6O_{18}P_6$) was used for sample dispersion.

Mineralogy of the clay fraction (<2 μm) was determined using powder X-ray diffraction (P-XRD, Cubix[3], Malvern Panalytical, Almelo, Netherlands). Prior to analysis, samples were treated with hydrochloric acid (HCl) to remove OM. P-XRD was performed on random powder samples and on oriented samples after saturation with Ca^{2+} and ethylene glycol (room temperature) and K^+ (room temperature and stepwise heated to 550 °C).

2.3. Physical fractionation

We followed a modified density and particle size fractionation scheme of Kölbl and Kögel-Knabner (2004) and Steffens et al. (2009) to separate POM and MAOM fractions from bulk soils. A detailed description of the fractionation procedure can be found in Mayer et al. (2022). Briefly, POM fractions (>20 μm), i.e. free particulate OM (fPOM) and occluded particulate OM (oPOM), were separated via density fractionation in a Na-polytungstate solution ($\rho = 1.8$ g cm^{-3}) before and after aggregate disruption through ultrasonication (200 J ml^{-1}), from 30 g of air-dried bulk soil (<2 mm). The remaining mineral fraction was rinsed salt-free and separated by wet sieving and sedimentation in Atterberg cylinders to yield the fine silt and clay-sized MAOM fraction (<6.3 μm) (Mueller et al., 2014).

All separated SOM fractions were air-dried at 60 °C, ground and analyzed in duplicate for total C concentrations via dry combustion on a Vario EL cube elemental analyzer (Elementar Analysensysteme, Hanau, Germany). As bulk samples were free of carbonates, the total C concentration equals the organic C concentration.

2.4. Specific surface area analysis

We measured the specific surface area (SSA) of the MAOM fraction from 1982 to 2017 by multiple-point BET (Brunauer et al., 1938) adsorption of N_2 at 77 K, using the BELSORP®-miniX surface area and pore size distribution analyzer (Microtrac MRB, USA/Japan/Germany), each before ($SSA_{untreated}$) and after removal of OM (SSA_{NaOCl}). Prior to measurement, samples were outgassed for 6–12 h under vacuum at 75 °C. After $SSA_{untreated}$ measurement, OM was removed from the same samples following a modified method of Kaiser et al. (2002) and Zimmermann et al. (2007). Briefly, 0.7–1 g of sample was oxidized during 18 h at room temperature (25 °C) with 6% sodium hypochlorite (NaOCl). We adjusted the solution to pH 8 with concentrated hydrochloric acid (HCl), at a soil-to-solution ratio of 1:50 (wt/wt). The samples were then centrifuged at 2000 g for 30 min and rinsed with deionized water until <50 μS cm^{-1}. OM oxidation and rinsing was repeated three times. Afterwards the SSA was determined again for the treated samples (SSA_{NaOCl}).

2.5. Radiocarbon analysis

The ^{14}C activity of OC in the separated MAOM fraction (<6.3 μm) of all plots and sampled years ($n = 16 \times 6 = 96$) was measured with accelerator mass spectrometry (AMS) at the Laboratory for the Analysis of Radiocarbon with AMS (LARA) at the University of Bern (Szidat et al., 2014). Without any further chemical treatment, roughly 30 mg of ground and homogenized sample material ($\cong 1$ mg C) was combusted in an elemental analyzer (Vario Micro Cube, Elementar Analysensysteme, Hanau, Germany), transformed into solid targets using an automated graphitization equipment (AGE), and measured with the MIni CArbon DAting System MICADAS (Synal et al., 2007). Each AMS measurement included multiple OxII radiocarbon standards (NIST, SRM 4990 C) and

fossil sodium acetate samples for normalization and correction of blanks as well as isotopic fractionations.

2.5.1. Mean residence time (MRT) of MAOM

The mean residence time (MRT) of MAOM was calculated using a ^{14}C model that takes into account 'bomb ^{14}C' and radioactive decay (Conen et al., 2008; Mueller et al., 2014). First, we determined the ^{14}C activity (Fraction Modern; F^{14}C) of OC, following the approach of Harkness et al. (1986):

$$A_t = A_{(t-1)} * e^{-k} + (1 - e^{-k}) * A_i - A_{(t-1)} * \lambda \tag{1}$$

where A_t is the measured ^{14}C activity in MAOM at time t, i.e. the respective year of soil sampling, corrected for radioactive decay until the year of ^{14}C measurement (2021). $A_{(t-1)}$ is the ^{14}C activity of SOM in the year preceding sampling, k the exchange rate of OC in MAOM (i.e. 1/MRT), and λ the ^{14}C decay constant (1/8268 yr^{-1}). A_i is the ^{14}C activity within the atmosphere and is composed of data from Reimer et al. (2020) (1511–1950) and Hua et al. (2022) (1950–2017).

A fundamental requirement of the model is the steady-state condition of the investigated fraction, i.e. balanced C inputs and outputs. In BIODYN and CONFYM, the MAOM-C content was in steady-state from 1982 to 2017, and in CONMIN and NOFERT from 1989 to 2017 and from 2003 to 2017, respectively (Supplementary Table 4). This meant that MRTs had to be estimated based on ^{14}C activities of different periods within the farming systems. Therefore, we additionally used the period from 2003 to 2017, during which MAOM-C contents of all farming systems were in steady-state.

We calculated the MRT of OM in MAOM according to equation (1) by repeatedly adjusting the MRT until the root-mean-square error (RMSE) between the calculated A_i at the chosen MRT and the measured ^{14}C activity at the corresponding sampled years reached the minimum. However, there is an unknown time difference between C assimilation by the crop and OM incorporation into MAOM (i.e. time lag). Therefore, we tested different time lags (0, 5 and 10 years), to account for the change in ^{14}C signal of the incoming OM caused by radioactive decay during this period, which affects the estimation of the MRT.

2.5.2. C turnover rates within MAOM

We calculated the annual C turnover rate in MAOM (mg g^{-1} yr^{-1}) for each plot by dividing the mean MAOM-C content (mg g^{-1}) during steady-state periods (NOFERT: 2003–2017, CONMIN: 1989–2017, CONFYM and BIODYN: 1982–2017) by the estimated MRT. In addition, we multiplied the annual MAOM-C turnover rate of each plot with its soil volume per hectare (0–20 cm depth) (using bulk densities of CRP 1, assuming its consistency over time (Leifeld et al., 2009)) to obtain values in a physical unit relevant to practice (kg C ha^{-1} yr^{-1}).

2.6. Statistical analyses

We used a one-way ANOVA in RStudio (R version 4.1.2.; RStudio Team (2021)) to identify statistically significant differences between farming systems for SSA, estimated MRTs and turnover rates. Prior to the ANOVA, residuals were tested for normal distribution using the Shapiro-Wilk test and visual inspection of QQ-plots, and homogeneity of variances was tested using Levene's test. Subsequently, a post-hoc Tukey HSD test was performed using a significance level of $\alpha = 0.05$, for all tests.

We applied a linear mixed effects model with repeated measurements to determine the impact of farming systems on ^{14}C activities and OC removal (i.e. oxidation-resistant and removable OC) as a function of sampling year. In short, the lme function of the nlme package was used (Pinheiro et al., 2020) with farming system nested in subplot and column as repeated random factors to account for spatial heterogeneity within the experimental design of the DOK trial. A two-way ANOVA was then employed to determine the impact of farming system, sampling

year and their interaction on ^{14}C activities. Residuals were tested for normal distribution using the Shapiro-Wilk test and visual inspection of QQ-plots, and homogeneity of variances was tested using Levene's test. Subsequently, a post-hoc Tukey HSD test was performed using a significance level of $\alpha = 0.05$, to test for differences between the farming systems.

3. Results

3.1. Clay content, mineralogy and development of MAOM-C contents

Clay content (<2 μm) was similar between all farming systems and averaged $21.5 \pm 3.2\%$. Clay mineralogy was dominated by 2:1 phyllosilicates, i.e. Illite ($12.6 \pm 3.1\%$) and Smectite ($3.7 \pm 1.7\%$) (Table 1). Within NOFERT, CONMIN and BIODYN there was one plot each (plot 93, 94 and 88) that had higher clay contents and Illite and/or Smectite contents compared to the other three plot replicates within the farming system.

Detailed results on the distribution of C between the separated fractions and their temporal development can be found in Mayer et al. (2022). In BIODYN and CONFYM, MAOM-C contents remained stable over the whole observation period (Supplementary Table 4). In CONMIN, MAOM-C contents decreased by 14% from 1982 to 1989, but remained stable thereafter. In NOFERT, MAOM-C contents decreased by 27% from 1982 to 2003, but remained stable thereafter. Throughout the whole observation period, CONFYM and CONMIN had similar MAOM-C levels. The only significant differences in MAOM-C contents were measured between BIODYN and NOFERT from 2003 onwards.

3.2. Specific surface area analysis

In 1982, $SSA_{untreated}$ of MAOM was similar in all farming systems, averaging 17.1 ± 1.8 m^2 g^{-1} (Fig. 1 and Table 2). $SSA_{untreated}$ remained constant in 2017 in all farming systems except NOFERT, where it increased significantly. This increase occurred only when excluding an extreme outlier (plot 93, marked with asterisk in Fig. 1), which showed a strong decrease of -6.2 m^2 g^{-1} from 1982 to 2017 and had by far the highest clay content (24.8%) compared to the other NOFERT plots (Table 1).

Across all plots and years, the efficiency of OC removal as the relative proportion of initial OC in MAOM ranged from 62 to 82% which is
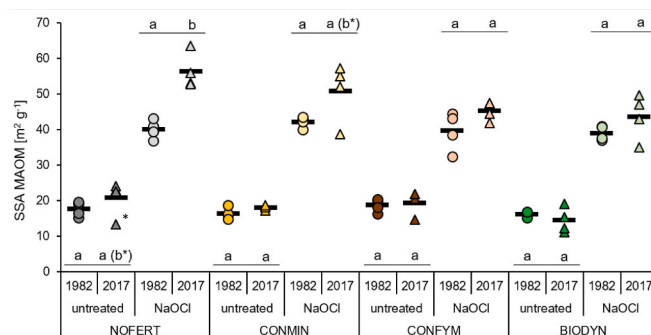

Fig. 1. Specific surface area (SSA) of MAOM determined by multiple-point BET adsorption of N$_2$. Symbols show single plot replicates (n = 4) for each farming system from the first year (1982, circles) and last year of sampling (2017, triangles). Dark and light shades show untreated samples and samples after OC removal with NaOCl, respectively, color-coded according to each farming system. Black bars represent the mean of 4 plot replicates and post-hoc Tukey letters give significant differences at p < 0.05. Single plot replicates with asterisks are outliers within the farming systems. Post-hoc Tukey letters in brackets give the significant differences when excluding outliers.

consistent with results of other studies that also used NaOCl (Helfrich et al., 2007; Mikutta and Kaiser, 2011; Mikutta et al., 2005). In 1982, the average OC removal via NaOCl was 5.4 ± 0.8 mg g^{-1} (= $69.5 \pm 2.8\%$ of total MAOM-C) with no significant differences between the farming systems (Fig. 2 and Table 2). The amount of oxidation-resistant OC was also similar across farming systems. The removal of OC significantly increased the measured SSA (SSA_{NaOCl}) by 22.99 m^2 g^{-1} on average to a mean of 40.1 ± 3.2 m^2 g^{-1}, with no significant differences among farming systems.

In 2017, oxidation-resistant OC significantly decreased in NOFERT and slightly decreased in CONMIN, compared to 1982. In CONFYM and BIODYN, the amount of oxidation-resistant OC remained unchanged from 1982 to 2017 (Fig. 2 and Table 2). SSA_{NaOCl} increased significantly more than after NaOCl treatment in 1982 ($+30.8$ m^2 g^{-1}) to an average of 48.9 ± 7.4 m^2 g^{-1} across all systems (Fig. 1 and Table 2).

Per milligram OC removed by NaOCl, an average of 4.4 ± 0.9 m^2 of SSA was exposed in 1982, with no significant differences between farming systems (Table 2). In 2017, the SSA exposed per milligram of

Table 1
Overview of clay characteristics of all 16 observed plots, measured on bulk soil samples from 2019. Values in bold indicate mean values and standard deviations of the 4 plots per farming system. A one-way ANOVA revealed no significant differences between any of the farming systems for any parameter.

farming system	plot	clay (<2 μm) [%]	phyllosilicates [%]	2:1 Illite [%]	Smectite [%]	Chlorite [%]	1:1 Kaolinite [%]
NOFERT	3	19.5	21.6	11.7	4.6	4.3	1.0
	37	15.5	18.0	10.9	2.7	3.5	0.9
	59	21.1	18.6	11.3	2.7	4.5	0.1
	93	24.8	21.7	8.6	7.3	2.7	3.0
		20.2 ± 3.4	**20.0 ± 2.0**	**10.6 ± 1.4**	**4.3 ± 2.2**	**3.8 ± 0.8**	**1.3 ± 1.2**
CONMIN	4	21.9	20.8	12.9	3.1	2.9	1.9
	38	20.7	19.4	10.9	4.2	2.0	2.3
	60	19.9	15.7	8.0	4.1	1.8	1.9
	94	24.3	26.3	16.9	3.9	4.3	1.3
		21.7 ± 1.9	**20.6 ± 4.4**	**12.2 ± 3.7**	**3.8 ± 0.5**	**2.8 ± 1.1**	**1.9 ± 0.4**
CONFYM	22	21.4	17.5	11.4	2.5	3.2	0.4
	32	16.5	21.0	14.7	2.6	3.1	0.6
	66	22.4	20.4	14.1	2.4	3.7	0.3
	76	21.2	21.5	14.4	2.6	3.4	1.1
		20.4 ± 2.6	**20.1 ± 1.8**	**13.7 ± 1.5**	**2.5 ± 0.1**	**3.4 ± 0.3**	**0.6 ± 0.4**
BIODYN	10	21.7	24.7	12.1	7.6	2.4	2.6
	44	21.7	17.5	11.5	2.1	2.0	1.9
	54	21.3	16.9	11.5	1.8	2.2	1.4
	88	29.3	31.5	21.0	4.2	2.6	3.7
		23.5 ± 3.9	**22.7 ± 6.9**	**14.0 ± 4.7**	**3.9 ± 2.7**	**2.3 ± 0.3**	**2.4 ± 1.0**

Table 2

Overview of OC removal efficiency and SSA analyses of each farming system for the first year (1982) and last year of observation (2017), before ($SSA_{untreated}$) and after (SSA_{NaOCl}) treatment with NaOCl. SSA_{NaOCl} - $SSA_{untreated}$ corresponds to the mineral surface area exposed after OC removal and $\Delta SSA/OC$ removed corresponds to the mineral surface area exposed per mg of OC removed. The values correspond to the mean of n = 4 plots per farming system and their standard deviation. Significant differences between systems at p < 0.05 are indicated by post-hoc Tukey letters. Post-hoc Tukey letters in brackets give the significant differences excluding outliers.

| year	farming system	OC removal [mg g^{-1}]	[%]	oxidation-resistant OC [mg g^{-1}]	$SSA_{untreated}$ [m^2 g^{-1}]	SSA_{NaOCl} [m^2 g^{-1}]	SSA_{NaOCl} - $SSA_{untreated}$ [m^2 g^{-1}]	$\Delta SSA/OC$ removed [m^2 mg^{-1}]
1982	**NOFERT**	5.45 ± 0.70 a	72.1 ± 2.2	2.13 ± 0.47 a	17.47 ± 2.06 a	39.89 ± 2.67 a	22.42 ± 2.93 a	4.19 ± 0.93 a
	CONMIN	5.52 ± 0.94 a	70.3 ± 2.1	2.34 ± 0.45 a	16.28 ± 1.64 a	42.01 ± 1.52 a	25.73 ± 2.47 a	4.73 ± 0.75 a
	CONFYM	4.84 ± 0.41 a	68.7 ± 2.2	2.23 ± 0.43 a	18.56 ± 1.90 a	39.48 ± 5.54 a	20.92 ± 3.60 a	4.39 ± 1.10 a
	BIODYN	5.57 ± 1.21 a	66.8 ± 2.3	2.76 ± 0.55 a	16.00 ± 0.71 a	38.90 ± 2.02 a	22.90 ± 1.55 a	4.28 ± 1.11 a
2017	**NOFERT**	4.37 ± 0.34 a	79.0 ± 2.4	1.18 ± 0.25 a	20.62 ± 4.95 a (a*)	56.19 ± 5.02 a (a*)	35.56 ± 9.77 a	8.11 ± 1.93 a
	CONMIN	4.97 ± 0.46 ab	73.8 ± 2.7	1.78 ± 0.38 ab	17.97 ± 0.58 a (ab*)	50.62 ± 8.28 a (a*)	32.65 ± 8.60 a	6.71 ± 2.20 a
	CONFYM	4.61 ± 0.19 ab	67.3 ± 4.9	2.26 ± 0.47 bc	19.18 ± 3.21 a (ab*)	45.11 ± 2.70 a (b*)	25.93 ± 4.87 a	5.61 ± 1.00 a
	BIODYN	5.60 ± 0.99 b	67.1 ± 2.6	2.73 ± 0.32 c	14.34 ± 3.51 a (b*)	43.51 ± 6.40 a (b*)	29.17 ± 9.89 a	5.42 ± 2.18 a
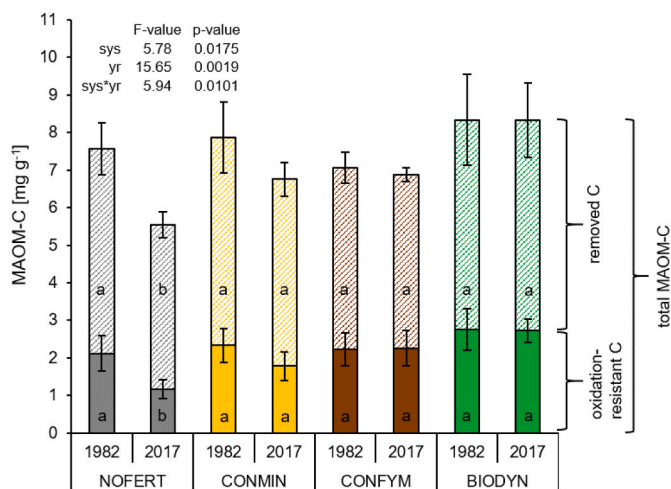
Fig. 2. Efficiency of C removal in MAOM in all farming systems via treatment with NaOCl for the first (1982) and last year (2017) of observation. Filled columns show the C proportion that was not removed by NaOCl, i.e. resistant to oxidation, and shaded columns show the C proportion that was removed by NaOCl. Error bars show the standard deviation of the individual plots (n = 4) per farming system. Results of a repeated two-way ANOVA (sys = farming system, yr = year) are depicted, using a linear mixed effect model that accounts for the spatial arrangement of plots within the experimental design. Post-hoc Tukey letters give significant differences between 1982 and 2017 at p < 0.05.

removed OC increased to a mean of 6.5 ± 2.0 m^2 (NOFERT: +3.9, CONMIN: +2.0, CONFYM: +1.2 and BIODYN: +1.1 m^2 mg^{-1}) with significant increases in NOFERT.

3.3. Carbon mean residence times

In all farming systems, the average ^{14}C activity of MAOM (Fraction Modern, F^{14}C) significantly decreased from 1.0589 in 1982 to 1.0205 in 2017, and was significantly affected by sampling year and farming system (Fig. 3). It is noticeable that systems without organic fertilizer (NOFERT and CONMIN) and systems with organic fertilizer application (CONFYM and BIODYN) show significantly different ^{14}C activities from 1996 onwards. On average, ^{14}C activity was 0.0214 F^{14}C higher in
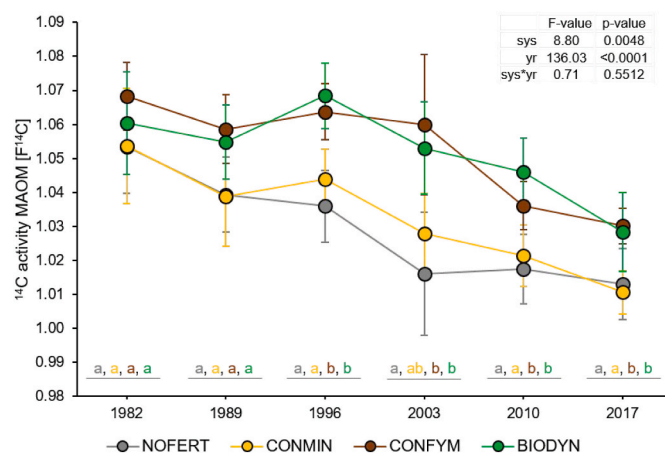

Fig. 3. ^{14}C activity, given in Fraction Modern (F^{14}C) measured within MAOM for all farming systems and sampled years. Circles show farming system means and the error bars show the standard deviation of single plot replicates (n = 4) per farming system. Results of a repeated two-way ANOVA (sys = farming system, yr = year) are depicted, using a linear mixed effect model that accounts for the spatial arrangement of plots within the experimental design. Post-hoc Tukey letters give significant differences at p < 0.05.

CONFYM and BIODYN compared to CONMIN and NOFERT.

The basic model requirement for the MRT estimation was the steady-state condition of MAOM. We had to choose a time lag (between C assimilation by the crop until incorporation in MAOM) and a period for the estimation of MRT (steady-state period for each individual farming system, or due to better comparability, the steady-state period of NOFERT (2003–2017) for all farming systems). Estimated MRT were found to be robust in a sensitivity analysis, regarding the order of farming systems for all tested time lags and periods (Supplementary Fig. 2 and Supplementary Table 5). The 10-yr time lag was excluded due to high RMSE (steady-state: 0.0194, 2003–2017: 0.0242). The 0-yr time lag had relatively low RMSE (steady-state: 0.0133, 2003–2017: 0.0098), but would imply that there was no temporal offset between C assimilation by the crop and incorporation of OM into MAOM, which is unlikely and would affect the MRT estimation. Finally, we chose a 5-yr time lag and the individual steady-state periods of the farming systems (Supplementary Table 5) to account for higher amounts of observations (steady-

state: n = 80, 2003–2017: n = 48) instead of minimal improvements in model accuracy (RMSE; steady-state: 0.0107, 2003–2017: 0.0102). The estimated MRTs of MAOM averaged 178 ± 49 yrs across all farming systems and were significantly higher in NOFERT (238 ± 40 yrs) and CONMIN (195 ± 27 yrs), compared to CONFYM (138 ± 18 yrs) and BIODYN (140 ± 19 yrs) (Fig. 4a).

We identified one outlier plot in both, NOFERT an CONMIN (marked with an asterisk in Fig. 4a). The NOFERT outlier (plot 37) had a significantly lower clay content (15.5%), as well as the lowest calculated MRT compared to the other NOFERT plots. In contrast, the CONMIN outlier (plot 94) had the highest clay content (24.3%), as well as the highest calculated MRT, compared to the other CONMIN plots. In addition, we observed a positive correlation between the calculated MRT and clay content, especially for farming systems not receiving organic fertilizers (R^2: NOFERT = 0.85, CONMIN = 0.83) (Fig. 5a). We also found a strong positive correlation between the estimated MRT and smectite contents (Fig. 5b).

3.4. Carbon turnover rates within MAOM

The amount of MAOM-C that passes annually through this fraction during steady-state periods averaged 0.043 mg C g^{-1} yr^{-1}. It was lowest in NOFERT (0.024 ± 0.003 mg C g^{-1} yr^{-1}), followed by CONMIN (0.034 ± 0.003 mg C g^{-1} yr^{-1}), CONFYM (0.051 ± 0.009 mg C g^{-1} yr^{-1}) and highest in BIODYN (0.059 ± 0.004 mg C g^{-1} yr^{-1}) (Fig. 4b, **bottom right**). We found no significant differences between CONFYM and BIODYN, but their C turnover was significantly higher than in CONMIN and NOFERT, and significantly higher in CONMIN than in NOFERT. This corresponded to an average annual C mass flow rate in MAOM of 111 kg C ha^{-1} yr^{-1} (0–20 cm) across farming systems (NOFERT: 62 ± 8 < CONMIN: 91 ± 6 < CONFYM: 137 ± 22 < BIODYN: 155 ± 11 kg C ha^{-1} yr^{-1}) (Fig. 4b).

4. Discussion

4.1. Best preconditions for MAOM-C stabilization under organic fertilization

In 1982, oxidation of OM with NaOCl resulted in an equal increase of SSA_{NaOCl} (Fig. 1) and similar amounts of oxidation-resistant C (Fig. 2) in all farming systems. In 2017, SSA_{NaOCl} significantly increased in NOFERT and CONMIN (Fig. 1), and oxidation-resistant C significantly decreased in NOFERT, compared to treated samples from 1982 (Table 2 and Fig. 2). This suggests that 36 years of arable farming negatively affected the stability of OM in MAOM in these systems.

Oxidation-resistant C is typically found in organo-mineral associations (Eusterhues et al., 2003; Mikutta et al., 2006), i.e. building units of

microaggregates (Totsche et al., 2018). Microaggregates are formed within macroaggregates (Oades and Waters, 1991). Therefore, macroaggregate formation and turnover is a major determinant of MAOM stability (Six et al., 2000), but is negatively influenced by tillage and harvesting practices (Mayer et al., 2022). Organic fertilization in BIODYN and CONFYM significantly increased the microbial activity (Krause et al., 2022), which led to increased aggregate formation, relative to NOFERT and CONMIN (Mayer et al., 2022). In BIODYN and CONFYM, this resulted in unchanged amounts of oxidation-resistant MAOM-C at higher levels than in CONMIN and NOFERT, where oxidation resistant MAOM-C was reduced from 1982 to 2017 (Fig. 2).

NaOCl treatment increased the exposure of mineral surface area per mg of destroyed OC in 2017, compared to treated samples in 1982 (Table 2). In BIODYN (5.42 ± 2.18 m² g^{-1}) and CONFYM (5.61 ± 1.00 m² g^{-1}), less SSA was exposed compared to CONMIN (6.71 ± 2.20 m² g^{-1}) and the significant increase in NOFERT (8.11 ± 1.93 m² g^{-1}) (Table 2). These results indicate a reduced aggregate stability, especially under low OM inputs (i.e. NOFERT and CONMIN), which allowed NaOCl to increasingly enter and break up previously more stable aggregates, exposing surface areas that were not accessible in 1982. In addition, this could indicate a shift of C sorption from organo-organic associations (i.e. C patches) to organo-mineral associations (i.e. directly on the mineral surface) (Kleber et al., 2015; Vogel et al., 2014) in CONMIN and NOFERT. In BIODYN and CONFYM however, new OM from fertilizers might preferentially form patchy organo-organic assemblages, where OM is already present (Possinger et al., 2020; Vogel et al., 2014). Therefore, we assume that in systems with regular OM supply via organic fertilization, its stabilization in MAOM is largely decoupled from the availability of free binding sites on fine mineral particle surfaces (Schweizer et al., 2018).

It is noteworthy, that the qualitative differences between the applied organic fertilizers (BIODYN = composted manure; CONFYM = stacked manure) did not affect OM stabilization in MAOM (Figs. 1 and 2 and Supplementary Table 4). This was despite the relative enrichment of BIODYN compost with more recalcitrant plant-derived OM and microbial degradation products due to the higher losses of labile C compounds during aerobic composting (Fließbach and Mäder, 2000), compared to stacked manure in CONFYM. Previous fractionation results with the same samples showed significant differences in POM quantity and aggregate stability between these two systems as a consequence of different fertilizer qualities (Mayer et al., 2022). This could have affected MAOM-forming processes via more direct contacts between organic fertilizers and mineral surfaces. We assume that (1.) the qualitative differences were too subtle (C/N 17 in BIODYN vs. 23 in CONFYM); and (2.) the differences were neutralized during the transition from the POM to the MAOM fraction.

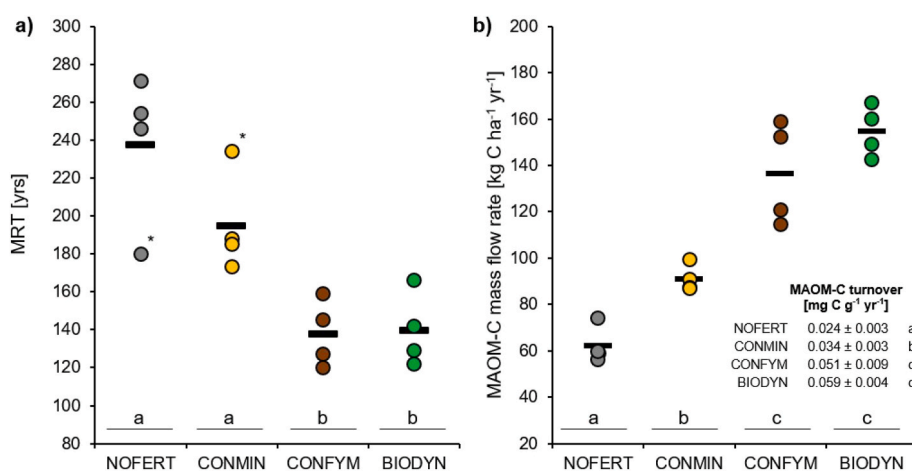In addition, avoiding the use of mineral fertilizers and pesticides in

Fig. 4. a) Estimated mean residence times (MRT, yrs) of MAOM for each farming system (5-yr time lag) and (b) annual C mass flow rate (kg C ha^{-1} yr^{-1}) during steady-state periods within each farming system (NOFERT: 2003–2017, CONMIN: 1989–2017, CONFYM and BIODYN: 1982–2017). The black bars represent the mean values per farming system of n = 4 individual plot replicates, depicted as colored circles. Post hoc Tukey letters give significant differences at p < 0.05 between farming systems after one-way ANOVA. Single plot replicates marked with an asterisk show outliers.
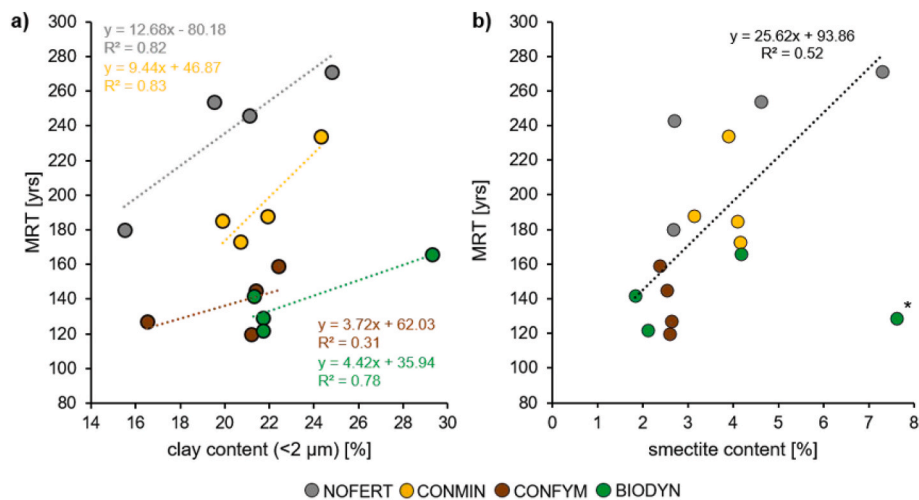
Within figure b:

MAOM-C turnover [mg C g^{-1} yr^{-1}]

NOFERT	0.024 ± 0.003	a
CONMIN	0.034 ± 0.003	b
CONFYM	0.051 ± 0.009	c
BIODYN	0.059 ± 0.004	c

Fig. 5. Correlation of estimated MRT (yrs) of MAOM with (a) clay content (<2 μm) and (b) smectite content. Circles show the single plot replicates and dotted lines show the linear trends of circles colored according to the respective farming system. In (b), the linear trend over all plots is shown, excluding the outlier marked with an asterisk.

BIODYN, which affect soil microbial community structure (Hartmann et al., 2015), also had no positive effect on OM stabilization in MAOM, compared to CONFYM.

Overall, the constant supply of OM through organic fertilizers in BIODYN and CONFYM initiates an improved aggregate stability and different sorption mechanisms of OM to fine mineral surfaces, compared to CONMIN and NOFERT. Therefore, our hypothesis that organic fertilization would lead to increased stabilization of MAOM, is true.

4.2. Dynamic stability of MAOM-C - highest contents despite highest turnover under organic fertilization

We expected higher MRTs and lower turnover of MAOM under organic fertilization, because of the supposedly higher stability of MAOM-C in BIODYN and CONFYM (i.e. enhanced aggregation, higher oxidation resistance (Fig. 2)) compared to CONMIN and NOFERT. However, MRTs of MAOM were significantly higher in NOFERT (238 ± 40 yrs) and CONMIN (195 ± 27 yrs), compared to CONFYM (138 ± 18 yrs) and BIODYN (140 ± 19 yrs) (Fig. 4a). These results were surprising given the fact that chemical oxidation with NaOCl has been shown to leave C with significantly higher ages and MRTs (Jagadamma et al., 2010; Kleber et al., 2005; Kögel-Knabner et al., 2008). This shows that chemical methods are of limited use in differentiating the stability of OM to biodegradation (Mikutta and Kaiser, 2011).

In BIODYN and CONFYM, the increased microbial activity (Krause et al., 2022) ensured a faster processing of the steady high supply of young OM from organic fertilizers. This led to an increased accumulation of young microbial degradation products in MAOM, significantly shorter MRTs (-78 yrs) (Fig. 4a) and significantly higher annual C mass flow rates in MAOM ($+70$ kg C ha^{-1} yr^{-1}) (Fig. 4b), compared to NOFERT and CONMIN. The amount of MAOM-C in BIODYN and CON-FYM remained constant over the 36-year period from 1982 to 2017 (Fig. 2 and Supplementary Table 4). This implies that the faster turnover of MAOM-C in BIODYN and CONFYM (factor 1.7) is compensated by the even greater OM input rates (factor 2.3), resulting in higher MAOM-C contents, relative to NOFERT and CONMIN.

The omission of additional OM inputs via fertilization in NOFERT and CONMIN resulted in a high spatial substrate heterogeneity (Lehmann et al., 2020; Shi et al., 2021), reducing the likeliness for the spatial co-occurrence of MAOM and decomposers (Don et al., 2013). The unchanged ^{14}C activity in MAOM during the steady-state period in NOFERT (2003–2017) (Fig. 3) illustrates these low OM inputs of which very little was incorporated into MAOM over this period. As a result, a

small, old OM fraction was isolated and preserved that turned over much slower, resulting in longer MRTs compared to CONFYM and BIODYN (Fig. 4a). The fact that the older MAOM in NOFERT had significantly lower aromatic C than younger MAOM in BIODYN (Mayer et al., 2022), supports the assumption that its reduced turnover and longer MRT resulted from the spatial isolation from its decomposers and not due to its recalcitrance to microbial degradation. This is in line with findings of Kleber et al. (2011), who showed that OM with the highest ^{14}C age (i.e. highest MRTs) had an easily metabolizable chemical composition.

We found no quantitative increase in MAOM-C of BIODYN and CONFYM over the 36-year period despite high OM inputs (Supplementary Table 4). This underlines that direct management of MAOM-C is not possible. Using the empirical formulas of Hassink (1997) and Wiesmeier et al. (2015), Mayer et al. (2022) showed high C saturation deficits of the fine fraction (<20 μm) for all farming systems. Thus, C saturation is not an explanation for the lack of MAOM-C enrichment. Furthermore, the ^{14}C data of this study show the continuous rejuvenation of MAOM with new OM across all farming systems (Fig. 3), contradicting that the 36-year period was too short for the incorporation of new OM in MAOM. Imaging techniques could provide further insight into the mechanistic processes that control and/or limit the accumulation of OM within MAOM at the submicron scale and improve our knowledge of how different fertilizer types might affect these processes (Steffens et al., 2017; Vogel et al., 2014).

Overall, we found MAOM-C to be more active in farming systems receiving organic fertilizers than in purely mineral and unfertilized systems, which was contrary to our hypothesis of longer MRTs in BIO-DYN and CONFYM. Just recently, attention has been drawn to the need for continuous turnover and microbial utilization of OM inputs to agricultural soils in order to maintain OM storage, aptly termed 'dynamic stability' by Dynarski et al. (2020). In our study, the 'dynamic stability' is manifested by the rapid and constant turnover of continuous OM inputs from composted (BIODYN) and stacked manure (CONFYM), and the subsequent stabilization of its degradation products in MAOM. This highlights the importance of maintaining continuous organic inputs in general, as a stop is anticipated to result in the fastest OM degradation in farming systems with high C turnover and short MRTs.

4.3. Clay content and clay mineralogy are crucial for OM stabilization - in the absence of organic fertilizers

We observed a strong positive correlation between clay content and the estimated MRT, especially in farming systems without organic

fertilization (Fig. 5a). This suggests that at low MAOM-C contents, clay content has greater influence on the stabilization (or 'retention') of OM than at higher MAOM-C contents. In the latter, OM sorption is less limited by vacant binding sites on mineral surfaces due to the preferable formation of organo-organo compounds (Possinger et al., 2020). Thus, the amount of clay particles is less critical for the stabilization of OM in CONFYM and BIODYN. In NOFERT and CONMIN, where MAOM-C contents are low, increased clay contents enhance the high spatial substrate heterogeneity (Lehmann et al., 2020; Shi et al., 2021) (see Chapter 4.2.) via stabilization and physical isolation of OM in aggregates, further reducing substrate availability to microbes and, as a result increase MAOM MRT.

Furthermore, we observed a positive correlation between smectite content and estimated MRT (Fig. 5b). Wattel-Koekkoek et al. (2003) identified clay mineralogy as the main factor explaining differences in MRT of OM, with the slowest turnover times in smectite-dominated soils. Smectite is an expendable 2:1 phyllosilicate with a high sorptive capacity due to its large SSA (Kleber et al., 2021; Saidy et al., 2013). The effect of smectite properties on MRT was stronger in NOFERT and CONMIN compared to CONFYM and BIODYN.

Notably, the outlier plots 88, 93, and 94 with the highest clay contents per farming system (Table 1), are directly adjacent in the DOK experimental design (Supplementary Fig. 1). This illustrates that at low SOM contents and in the absence of organic fertilization, even small clay content gradients at the field or plot level (NOFERT: 15–25%, CONMIN: 20–24%) (Table 2) can result in significant differences in MRT. For practice, this should raise awareness towards the fact that SOM turnover is also controlled by the heterogeneity of soil properties, particularly when OM inputs from fertilizers are missing. Consequently, exact knowledge about the heterogeneity of soil properties, e.g., through replicated and geolocated samplings, helps to minimize uncertainties in estimates of SOM persistence.

5. Conclusions

Using ^{14}C analysis and MRT estimation of the physically separated MAOM fraction (<6.3 µm), we demonstrated that constant organic fertilization resulted in significantly higher MAOM-C turnover and significantly shorter MRTs compared to non-organic fertilization over a 36-year period. Despite the highest MAOM-C turnover, MAOM-C contents were kept constant under organic fertilization, implying that the faster turnover is compensated by the high OM input rates. The results of this study illustrate that a constant supply and turnover of OM in mineral-associated fractions is vital to ensure the long-term stability of MAOM-C contents. However, we lack understanding on the sub-micron scale mechanisms that control C sequestration in MAOM explaining the limited accumulation of additional MAOM-C. This will improve the evaluation of the ability of agricultural soils to act as long-term C sinks. Overall, this study highlights the importance of the dynamic nature of organo-mineral interactions for SOM stabilization, especially in the context of advancing climate change. Supporting this dynamic nature of SOM via continuous organic fertilization and improving biological soil quality should therefore become the focus of sustainable and climate-friendly agriculture. This corroborates the theory of managing SOM rather than locking it away, which mixed farming systems that integrate livestock and arable farming are best suited for.

Funding

Declaration of competing interest

The authors declare that they have no known competing financial interests or personal relationships that could have appeared to influence the work reported in this paper.

Data availability

Data will be made available on request.

Acknowledgements

Appendix A. Supplementary data

Supplementary data to this article can be found online at https://doi.org/10.1016/j.soilbio.2023.109095.

References

Amelung, W., Bossio, D., de Vries, W., Kögel-Knabner, I., Lehmann, J., Amundson, R., Bol, R., Collins, C., Lal, R., Leifeld, J., Minasny, B., Pan, G., Paustian, K., Rumpel, C., Sanderman, J., van Groenigen, J.W., Mooney, S., van Wesemael, B., Wander, M., Chabbi, A., 2020. Towards a global-scale soil climate mitigation strategy. Nature Communications 11, 5427.

Barré, P., Fernandez-Ugalde, O., Virto, I., Velde, B., Chenu, C., 2014. Impact of phyllosilicate mineralogy on organic carbon stabilization in soils: incomplete knowledge and exciting prospects. Geoderma 235–236, 382–395.

Brunauer, S., Emmett, P.H., Teller, E., 1938. Adsorption of gases in multimolecular layers. Journal of the American Chemical Society 60, 309–319.

Bünemann, E.K., Bongiorno, G., Bai, Z., Creamer, R.E., De Deyn, G., de Goede, R., Fleskens, L., Geissen, V., Kuyper, T.W., Mäder, P., Pulleman, M., Sukkel, W., van Groenigen, J.W., Brussaard, L., 2018. Soil quality - a critical review. Soil Biology and Biochemistry 120, 105–125.

Chung, H., Grove, J.H., Six, J., 2008. Indications for soil carbon saturation in a temperate agroecosystem. Soil Science Society of America Journal 72, 1132–1139.

Conen, F., Zimmermann, M., Leifeld, J., Seth, B., Alewell, C., 2008. Relative stability of soil carbon revealed by shifts in δ^{15}N and C:N ratio. Biogeosciences 5, 123–128.

Cotrufo, M.F., Wallenstein, M.D., Boot, C.M., Denef, K., Paul, E., 2013. The Microbial Efficiency-Matrix Stabilization (MEMS) framework integrates plant litter decomposition with soil organic matter stabilization: do labile plant inputs form stable soil organic matter? Global Change Biology 19, 988–995.

de Vries, W., 2018. Soil carbon 4 per mille: a good initiative but let's manage not only the soil but also the expectations. Geoderma 309, 111–112.

Don, A., Rödenbeck, C., Gleixner, G., 2013. Unexpected control of soil carbon turnover by soil carbon concentration. Environmental Chemistry Letters 11, 407–413.

Dynarski, K.A., Bossio, D.A., Scow, K.M., 2020. Dynamic stability of soil carbon: reassessing the "permanence" of soil carbon sequestration. Frontiers in Environmental Science 8.

Eusterhues, K., Rumpel, C., Kleber, M., Kögel-Knabner, I., 2003. Stabilisation of soil organic matter by interactions with minerals as revealed by mineral dissolution and oxidative degradation. Organic Geochemistry 34, 1591–1600.

Feng, W., Plante, A.F., Six, J., 2013. Improving estimates of maximal organic carbon stabilization by fine soil particles. Biogeochemistry 112, 81–93.

Fließbach, A., Mäder, P., 2000. Microbial biomass and size-density fractions differ between soils of organic and conventional agricultural systems. Soil Biology and Biochemistry 32, 757–768.

Gattinger, A., Müller, A., Haeni, M., Skinner, C., Fließbach, A., Buchmann, N., Mäder, P., Stolze, M., Smith, P., El-Hage Scialabba, N., Niggli, U., 2012. Enhanced top soil carbon stocks under organic farming. Proceedings of the National Academy of Sciences 109, 18226–18231.

Gulde, S., Chung, H., Amelung, W., Chang, C., Six, J., 2008. Soil carbon saturation controls labile and stable carbon pool dynamics. Soil Science Society of America Journal 72, 605–612.

Harkness, D.D., Harrison, A.F., Bacon, P.J., 1986. The temporal distribution of 'bomb' ^{14}C in a forest soil. Radiocarbon 28, 328–337.

Hartmann, M., Frey, B., Mayer, J., Mäder, P., Widmer, F., 2015. Distinct soil microbial diversity under long-term organic and conventional farming. The ISME Journal 9, 1177–1194.

Hassink, J., 1997. The capacity of soils to preserve organic C and N by their association with clay and silt particles. Plant and Soil 191, 77–87.

Helfrich, M., Flessa, H., Mikutta, R., Dreves, A., Ludwig, B., 2007. Comparison of chemical fractionation methods for isolating stable soil organic carbon pools. European Journal of Soil Science 58, 1316–1329.

Hirte, J., Leifeld, J., Abiven, S., Mayer, J., 2018a. Maize and wheat root biomass, vertical distribution, and size class as affected by fertilization intensity in two long-term field trials. Field Crops Research 216, 197–208.

Hirte, J., Leifeld, J., Abiven, S., Oberholzer, H.-R., Mayer, J., 2018b. Below ground carbon inputs to soil via root biomass and rhizodeposition of field-grown maize and wheat at harvest are independent of net primary productivity. Agriculture, Ecosystems & Environment 265, 556–566.

Hua, Q., Turnbull, J.C., Santos, G.M., Rakowski, A.Z., Ancapichún, S., De Pol-Holz, R., Hammer, S., Lehman, S.J., Levin, I., Miller, J.B., Palmer, J.G., Turney, C.S.M., 2022. Atmospheric radiocarbon for the period 1950-2019. Radiocarbon 64, 723–745.

Jagadamma, S., Lal, R., Ussiri, D.A.N., Trumbore, S.E., Mestelan, S., 2010. Evaluation of structural chemistry and isotopic signatures of refractory soil organic carbon fraction isolated by wet oxidation methods. Biogeochemistry 98, 29–44.

Kaiser, K., Eusterhues, K., Rumpel, C., Guggenberger, G., Kögel-Knabner, I., 2002. Stabilization of organic matter by soil minerals - investigations of density and particle-size fractions from two acid forest soils. Journal of Plant Nutrition and Soil Science 165, 451–459.

Kleber, M., Bourg, I.C., Coward, E.K., Hansel, C.M., Myneni, S.C.B., Nunan, N., 2021. Dynamic interactions at the mineral-organic matter interface. Nature Reviews Earth & Environment 2, 402–421.

Kleber, M., Eusterhues, K., Keiluweit, M., Mikutta, C., Mikutta, R., Nico, P.S., 2015. Mineral-organic associations: formation, properties, and relevance in soil environments. Advances in Agronomy 130, 1–140.

Kleber, M., Mikutta, R., Torn, M.S., Jahn, R., 2005. Poorly crystalline mineral phases protect organic matter in acid subsoil horizons. European Journal of Soil Science 56, 717–725.

Kleber, M., Nico, P.S., Plante, A., Filley, T., Kramer, M., Swanston, C., Sollins, P., 2011. Old and stable soil organic matter is not necessarily chemically recalcitrant: implications for modeling concepts and temperature sensitivity. Global Change Biology 17, 1097–1107.

Kögel-Knabner, I., Guggenberger, G., Kleber, M., Kandeler, E., Kalbitz, K., Scheu, S., Eusterhues, K., Leinweber, P., 2008. Organo-mineral associations in temperate soils: integrating biology, mineralogy, and organic matter chemistry. Journal of Plant Nutrition and Soil Science 171, 61–82.

Kölbl, A., Kögel-Knabner, I., 2004. Content and composition of free and occluded particulate organic matter in a differently textured arable cambisol as revealed by solid-state ^{13}C NMR spectroscopy. Journal of Plant Nutrition and Soil Science 167, 45–53.

Kramer, M.G., Chadwick, O.A., 2018. Climate-driven thresholds in reactive mineral retention of soil carbon at the global scale. Nature Climate Change 8, 1104–1108.

Krause, H.-M., Fließbach, A., Mayer, J., Mäder, P., 2020. Implementation and management of the DOK long-term system comparison trial. In: Bhullar, G., Riar, A. (Eds.), Long-Term Farming Systems Research - Ensuring Food Security in Changing Scenarios. Elsevier, London, pp. 37–51.

Krause, H.-M., Stehle, B., Mayer, J., Mayer, M., Steffens, M., Mäder, P., Fliessbach, A., 2022. Biological soil quality and soil organic carbon change in biodynamic, organic, and conventional farming systems after 42 years. Agronomy for Sustainable Development 42.

Kundel, D., Bodenhausen, N., Jorgensen, H.B., Truu, J., Birkhofer, K., Hedlund, K., Mäder, P., Fliessbach, A., 2020. Effects of simulated drought on biological soil quality, microbial diversity and yields under long-term conventional and organic agriculture. FEMS Microbiology Ecology 96.

Kuzyakov, Y., Friedel, J.K., Stahr, K., 2000. Review of mechanisms and quantification of priming effects. Soil Biology and Biochemistry 32, 1485–1498.

Lal, R., 2010. Managing soils and ecosystems for mitigating anthropogenic carbon emissions and advancing global food security. BioScience 60, 708–721.

Lal, R., 2020. Soil organic matter and water retention. Agronomy Journal 112, 3265–3277.

Lal, R., Smith, P., Jungkunst, H.F., Mitsch, W.J., Lehmann, J., Nair, P.K.R., McBratney, A. B., de Moraes Sá, J.C., Schneider, J., Zinn, Y.L., Skorupa, A.L.A., Zhang, H.-L., Minasny, B., Srinivasrao, C., Ravindranath, N.H., 2018. The carbon sequestration potential of terrestrial ecosystems. Journal of Soil and Water Conservation 73, 145A–152A.

Lehmann, J., Hansel, C.M., Kaiser, C., Kleber, M., Maher, K., Manzoni, S., Nunan, N., Reichstein, M., Schimel, J.P., Torn, M.S., Wieder, W.R., Kögel-Knabner, I., 2020. Persistence of soil organic carbon caused by functional complexity. Nature Geoscience 13, 529–534.

Leifeld, J., Reiser, R., Oberholzer, H.-R., 2009. Consequences of conventional versus organic farming on soil carbon: results from a 27-year field experiment. Agronomy Journal 101, 1204–1218.

Mäder, P., Fließbach, A., Dubois, D., Gunst, L., Fried, P., Niggli, U., 2002. Soil fertility and biodiversity in organic farming. Science 296, 1694–1697.

Mayer, M., Krause, H.-M., Fliessbach, A., Mäder, P., Steffens, M., 2022. Fertilizer quality and labile soil organic matter fractions are vital for organic carbon sequestration in temperate arable soils within a long-term trial in Switzerland. Geoderma 426, 116080.

Mikutta, R., Kaiser, K., 2011. Organic matter bound to mineral surfaces: resistance to chemical and biological oxidation. Soil Biology and Biochemistry 43, 1738–1741.

Mikutta, R., Kleber, M., Jahn, R., 2005. Poorly crystalline minerals protect organic carbon in clay subfractions from acid subsoil horizons. Geoderma 128, 106–115.

Mikutta, R., Kleber, M., Torn, M.S., Jahn, R., 2006. Stabilization of soil organic matter: association with minerals or chemical recalcitrance? Biogeochemistry 77, 25–56.

Minasny, B., Malone, B.P., McBratney, A.B., Angers, D.A., Arrouays, D., Chambers, A., Chaplot, V., Chen, Z.-S., Cheng, K., Das, B.S., Field, D.J., Gimona, A., Hedley, C.B., Hong, S.Y., Mandal, B., Marchant, B.P., Martin, M., McConkey, B.G., Mulder, V.L., O'Rourke, S., Richer-de-Forges, A.C., Odeh, I., Padarian, J., Paustian, K., Pan, G., Poggio, L., Savin, I., Stolbovoy, V., Stockmann, U., Sulaeman, Y., Tsui, C.-C., Vågen, T.-G., van Wesemael, B., Winowiecki, L., 2017. Soil carbon 4 per mille. Geoderma 292, 59–86.

Mueller, C.W., Gutsch, M., Kothieringer, K., Leifeld, J., Rethemeyer, J., Brueggemann, N., Kögel-Knabner, I., 2014. Bioavailability and isotopic composition of CO_2 released from incubated soil organic matter fractions. Soil Biology and Biochemistry 69, 168–178.

Newcomb, C.J., Qafoku, N.P., Grate, J.W., Bailey, V.L., De Yoreo, J.J., 2017. Developing a molecular picture of soil organic matter-mineral interactions by quantifying organo-mineral binding. Nature Communications 8, 396.

Oades, J.M., Waters, A.G., 1991. Aggregate hierarchy in soils. Australian Journal of Soil Research 29, 815–828.

Paul, E.A., Follett, R.F., Leavitt, S.W., Halvorson, A., Peterson, G.A., Lyon, D.J., 1997. Radiocarbon dating for determination of soil organic matter pool sizes and dynamics. Soil Science Society of America Journal 61, 1058–1067.

Paustian, K., Larson, E., Kent, J., Marx, E., Swan, A., 2019. Soil C sequestration as a biological negative emission strategy. Frontiers in Climate 1, 1–11.

Paustian, K., Lehmann, J., Ogle, S., Reay, D., Robertson, G.P., Smith, P., 2016. Climate-smart soils. Nature 532, 49–57.

Pinheiro, J., Bates, D., DebRoy, S., Sarkar, D., Core Team, R, 2020. nlme: Linear and Nonlinear Mixed Effects Models. R package version 3.1-151. https://CRAN.R-pr oject.org/package=nlme.

Possinger, A.R., Zachman, M.J., Enders, A., Levin, B.D.A., Muller, D.A., Kourkoutis, L.F., Lehmann, J., 2020. Organo-organic and organo-mineral interfaces in soil at the nanometer scale. Nature Communications 11, 6103.

Rabot, E., Wiesmeier, M., Schlüter, S., Vogel, H.J., 2018. Soil structure as an indicator of soil functions: a review. Geoderma 314, 122–137.

Reimer, P.J., Austin, W.E.N., Bard, E., Bayliss, A., Blackwell, P.G., Bronk Ramsey, C., Butzin, M., Cheng, H., Edwards, R.L., Friedrich, M., Grootes, P.M., Guilderson, T.P., Hajdas, I., Heaton, T.J., Hogg, A.G., Hughen, K.A., Kromer, B., Manning, S.W., Muscheler, R., Palmer, J.G., Pearson, C., van der Plicht, J., Reimer, R.W., Richards, D.A., Scott, E.M., Southon, J.R., Turney, C.S.M., Wacker, L., Adolphi, F., Büntgen, U., Capano, M., Fahrni, S.M., Fogtmann-Schulz, A., Friedrich, R., Köhler, P., Kudsk, S., Miyake, F., Olsen, J., Reinig, F., Sakamoto, M., Sookdeo, A., Talamo, S., 2020. The IntCal20 northern hemisphere radiocarbon age calibration curve (0–55 cal kBP). Radiocarbon 62, 725–757.

Richner, W., Sinaj, S., 2017. Grundlagen für die Düngung landwirtschaftlicher Kulturen in der Schweiz (GRUD 2017), vol. 8. Agrarforschung Schweiz. Spezialpublikation, 276 S.

Riggers, C., Poeplau, C., Don, A., Frühauf, C., Dechow, R., 2021. How much carbon input is required to preserve or increase projected soil organic carbon stocks in German croplands under climate change? Plant and Soil 460, 417–433.

RStudio Team, 2021. RStudio. Integrated Development Environment for R. RStudio, PBC, Boston, MA. URL. http://www.rstudio.com/.

Saidy, A.R., Smernik, R.J., Baldock, J.A., Kaiser, K., Sanderman, J., 2013. The sorption of organic carbon onto differing clay minerals in the presence and absence of hydrous iron oxide. Geoderma 209–210, 15–21.

Sanderman, J., Hengl, T., Fiske, G.J., 2017. Soil carbon debt of 12,000 years of human land use. Proceedings of the National Academy of Sciences 114, 9575–9580.

Schmidt, M.W.I., Torn, M.S., Abiven, S., Dittmar, T., Guggenberger, G., Janssens, I.A., Kleber, M., Kögel-Knabner, I., Lehmann, J., Manning, D.A., Nannipieri, P., Rasse, D. P., Weiner, S., Trumbore, S.E., 2011. Persistence of soil organic matter as an ecosystem property. Nature 478, 49–56.

Schweizer, S.A., Hoeschen, C., Schlüter, S., Kögel-Knabner, I., Mueller, C.W., 2018. Rapid soil formation after glacial retreat shaped by spatial patterns of organic matter accrual in microaggregates. Global Change Biology 24, 1637–1650.

Shi, A., Chakrawal, A., Manzoni, S., Fischer, B.M.C., Nunan, N., Herrmann, A.M., 2021. Substrate spatial heterogeneity reduces soil microbial activity. Soil Biology and Biochemistry 152, 108068.

Six, J., Conant, R.T., Paul, E.A., Paustian, K., 2002. Stabilization mechanisms of soil organic matter: implications for C-saturation of soils. Plant and Soil 241, 155–176.

Six, J., Elliott, E.T., Paustian, K., 2000. Soil macroaggregate turnover and microaggregate formation: a mechanism for C sequestration under no-tillage agriculture. Soil Biology and Biochemistry 32, 2099–2103.

Steffens, M., Kölbl, A., Kögel-Knabner, I., 2009. Alteration of soil organic matter pools and aggregation in semi-arid steppe topsoils as driven by organic matter input. European Journal of Soil Science 60, 198–212.

Steffens, M., Kölbl, A., Schörk, E., Gschrey, B., Kögel-Knabner, I., 2011. Distribution of soil organic matter between fractions and aggregate size classes in grazed semiarid steppe soil profiles. Plant and Soil 338, 63–81.

Steffens, M., Rogge, D.M., Mueller, C.W., Höschen, C., Lugmeier, J., Kölbl, A., Kögel-Knabner, I., 2017. Identification of distinct functional microstructural domains

controlling C storage in soil. Environmental Science and Technology 51, 12182–12189.

Synal, H.-A., Stocker, M., Suter, M., 2007. MICADAS: a new compact radiocarbon AMS system. Nuclear Instruments and Methods in Physics Research Section B: Beam Interactions with Materials and Atoms 259, 7–13.

Szidat, S., Salazar, G.A., Vogel, E., Battaglia, M., Wacker, L., Synal, H.-A., Türler, A., 2014. 14C analysis and sample preparation at the new Bern Laboratory for the Analysis of Radiocarbon with AMS (LARA). Radiocarbon 56, 561–566.

Totsche, K.U., Amelung, W., Gerzabek, M.H., Guggenberger, G., Klumpp, E., Knief, C., Lehndorff, E., Mikutta, R., Peth, S., Prechtel, A., Ray, N., Kögel-Knabner, I., 2018. Microaggregates in soils. Journal of Plant Nutrition and Soil Science 181, 104–136.

Trumbore, S., 2009. Radiocarbon and soil carbon dynamics. Annual Review of Earth and Planetary Sciences 37, 47–66.

Vogel, C., Mueller, C.W., Höschen, C., Buegger, F., Heister, K., Schulz, S., Schloter, M., Kögel-Knabner, I., 2014. Submicron structures provide preferential spots for carbon and nitrogen sequestration in soils. Nature Communications 5, 2947.

von Lützow, M., Kögel-Knabner, I., Ekschmitt, K., Matzner, E., Guggenberger, G., Marschner, B., Flessa, H., 2006. Stabilization of organic matter in temperate soils: mechanisms and their relevance under different soil conditions - a review. European Journal of Soil Science 57, 426–445.

Wang, Y., Hsieh, Y.-P., 2002. Uncertainties and novel prospects in the study of the soil carbon dynamics. Chemosphere 49, 791–804.

Wattel-Koekkoek, E.J.W., Buurman, P., van der Plicht, J., Wattel, E., van Breemen, N., 2003. Mean residence time of soil organic matter associated with kaolinite and smectite. European Journal of Soil Science 54, 269–278.

Weil, R.R., Magdoff, F., 2004. Significance of soil organic matter to soil quality and health. In: Magdoff, F., Weil, R.R. (Eds.), Soil Organic Matter in Sustainable Agriculture. CRC Press, Boca Raton, pp. 1–43.

Wiesmeier, M., Munro, S., Barthold, F., Steffens, M., Schad, P., Kögel-Knabner, I., 2015. Carbon storage capacity of semi-arid grassland soils and sequestration potentials in northern China. Global Change Biology 21, 3836–3845.

Wiesmeier, M., Poeplau, C., Sierra, C.A., Maier, H., Frühauf, C., Hübner, R., Kühnel, A., Spörlein, P., Geuß, U., Hangen, E., Schilling, B., von Lützow, M., Kögel-Knabner, I., 2016. Projected loss of soil organic carbon in temperate agricultural soils in the 21st century: effects of climate change and carbon input trends. Scientific Reports 6, 32525.

WRB, I.W.G., 2015. World Reference Base for Soil Resources 2014, Update 2015 - International Soil Classification System for Naming Soils and Creating Legends for Soil Maps, vol. 106. World Soil Resources Reports No.

Zimmermann, M., Leifeld, J., Abiven, S., Schmidt, M.W.I., Fuhrer, J., 2007. Sodium hypochlorite separates an older soil organic matter fraction than acid hydrolysis. Geoderma 139, 171–179.